

1995121225

N95-27646

POINT DEFECT FORMATION IN OPTICAL MATERIALS EXPOSED TO THE SPACE ENVIRONMENT

J. L. Allen, N. Seifert, Y. Yao, R. G. Albridge, A. V. Barnes, N. H. Tolk
Center for Molecular and Atomic Studies at Surfaces
Department of Physics and Astronomy
Vanderbilt University
Nashville, TN 37235

A. M. Strauss
Department of Mechanical Engineering
Vanderbilt University
Nashville, TN 37235

R. C. Linton, R. R. Kamenetzky, J. A. Vaughn, and M. M. Finckenor
NASA Marshall Space Flight Center
MSFC, AL 35812

ABSTRACT

Point defect formation associated with early stages of optical damage was observed unexpectedly in two, and possibly three, different optical materials subjected to short-duration space exposure. Three calcium fluoride, two lithium fluoride, and three magnesium fluoride samples were flown on Space Shuttle flight STS-46 as part of the Evaluation of Oxygen Interactions with Materials - Third Phase experiment. One each of the calcium and magnesium fluoride samples was held at a fixed temperature of 60°C during the space exposure, while the temperatures of the other samples were allowed to vary with the ambient temperature of the shuttle cargo bay. Pre-flight and post-flight optical absorption measurements were performed on all of the samples. With the possible exception of the magnesium fluoride samples, every sample clearly showed the formation of F-centers in that section of the sample that was exposed to the low earth orbit environment. Solar vacuum ultraviolet radiation is the most probable primary cause of the defect formation; however, the resulting surface metallization may be synergistically altered by the atomic oxygen environment.

INTRODUCTION

The space environment offers many observational advantages over ground-based experiments. However, the low earth orbit (LEO) environment in which the space shuttle and other space systems operate has proven to be very harsh, having adverse effects on most exposed systems.¹⁻⁴ Because optical systems play a key role in many space experiments, a thorough understanding of the degradation of optical materials in a space environment is very important. To address this issue, the Vanderbilt University Center for Molecular and Atomic Studies at Surfaces (CMASS), in collaboration with NASA Marshall Space Flight Center, flew samples of calcium fluoride (CaF₂), lithium fluoride (LiF), and magnesium fluoride (MgF₂) on Space Shuttle flight STS-46 as part of the Evaluation of Oxygen Interactions with Materials - Third Phase (EOIM-III) experiment. As a result of the short duration space exposure during this flight,

point defect formation associated with the early stages of optical damage was unexpectedly observed in the CaF₂ and LiF samples. The space exposure also caused some effects in the MgF₂ samples that might be associated with F-center formation.

CaF₂, LiF, and MgF₂ are popular choices for lens and window materials in a wide variety of optical and infrared (IR) experiments, because of their excellent optical transmission properties from vacuum ultraviolet (VUV) to medium IR wavelengths (0.1 - 10 μm). It has been known for some time that ionizing radiation incident on alkali-halide and alkaline-earth-fluoride crystals creates hole defects, which may be highly mobile and lead to color center formation (F-center/H-center pairs), a process which is understood to be a precursor to darkening, surface metallization, erosion, and other optical damage phenomena.⁵⁻⁸ A single halogen ion vacancy that has trapped an electron is known as an F-center; an F₂-center is a pair of adjacent F-centers.

These defects give rise to optical absorption bands with well-characterized peak wavelengths. Table 1 summarizes the positions of the F- and F₂-band absorption maxima for the three materials studied.⁵⁻⁸

Table 1. *F-band absorption peak wavelengths.*⁵⁻⁸

Material	Peak wavelength (nm)	
	F - band	F ₂ - band
CaF ₂	370	370, 520
LiF	250	450
MgF ₂	260	370, 400

The CaF₂, LiF, and possibly the MgF₂ samples flown by CMASS/NASA on EOIM-III showed absorption peaks consistent with F-center formation as a result of the space exposure. The effects of space radiation on a wide variety of optical materials have been studied for many years in laboratory simulations and space experiments.⁹ While changes in optical absorption were seen in these studies, F-center defect formation due to space exposure has not been previously reported.

EXPERIMENT

The EOIM-III payload, which has been previously described in detail,¹⁰ contained a wide variety of experiments designed to meet its primary objective: production of benchmark atomic-oxygen-reactivity and induced-environment data. The experiment hardware included several passive sample carriers whose temperatures were allowed to vary with ambient temperature of the cargo bay. The hardware also contained three heated sample trays that were maintained at constant temperatures of 200, 120, and 60°C, during the EOIM-III Flight Operations portion of the flight.

As mentioned above, the CMASS/NASA experiment included a total of eight samples on the EOIM-III flight. Three more control samples (CaF₂-2, LiF-1, and LiF-3) were kept in the laboratory. All the samples are single crystal, parallel plane windows purchased from Infrared Optical Products, Inc. Table 2 summarizes the pertinent information about each flight sample. All of the 25-mm diameter samples were mounted in the EOIM-III trays with a 0.5 mm thick aluminum mask that covered approximately half of the sample surface. The three 12.5-mm samples were cut from original 25-mm diameter samples in order to facilitate post-flight Auger Electron Spectroscopy analysis of the samples. Two of these samples (LiF-4 and MgF₂-3) had to

be ground and polished after cutting. Unfortunately, this process increased the optical absorption and made the spectra dependent on sample orientation in the spectrophotometer with decreased reproducibility. However, as discussed below, the bulk defect formation due to space exposure was still observed in LiF-4.

Table 2. *List of flight samples.*

Sample	Nominal Diameter (mm)	Nominal Thickness (mm)	Mask	Tray
CaF ₂ -1	25	3	Yes	60°C
CaF ₂ -3	25	3	Yes	Passive
CaF ₂ -4	12.5	3	No	Passive
LiF-2	25	4	Yes	Passive
LiF-4	12.5	4	No	Passive
MgF ₂ -1	25	1	Yes	60°C
MgF ₂ -2	25	1	Yes	Passive
MgF ₂ -3	12.5	3	No	Passive

The EOIM-III experiment was flown on the STS-46 mission of the Space Shuttle Atlantis, July 31 - August 8, 1992.¹⁰ For the EOIM-III Flight Operations portion of the flight, the shuttle was maintained at an altitude of 123-124 nautical miles (nmi), or 228-230 km, for an exposure period of 42.25 hours with the cargo bay normal aligned (within +2°) with the orbital velocity vector (ram direction). During this period, the EOIM-III payload received an atomic oxygen fluence of $2.3 \pm 0.1 \times 10^{20}$ atoms/cm².¹¹

The STS-46 flight also included the European Space Agency Recoverable Satellite (EURECA), that was deployed and checked out at an altitude of 231 nmi (428 km) for an exposure period of 11.27 hours during which the cargo bay was pointed toward the sun. An additional 5.28 hours of exposure at 231 nmi occurred during EURECA release with the cargo bay in the ram direction. Atomic oxygen fluences during the 231 nmi exposure were 2-3 orders of magnitude less than those received during the 123-124 nmi exposure. However, it is very important to note that most of the EOIM-III samples, including the CMASS/NASA samples, were uncovered during the EURECA experiments. Consequently, they received a significant solar UV/VUV radiation dose, greater than that received during the rest of the mission. The solar UV/VUV flux as a function of energy was calculated using known orbit and solar parameters¹² and will be discussed below.

The optical absorption measurements were performed using a Hewlett-Packard 8452A Diode Array Spectrophotometer controlled by a PC Turbo AT microcomputer. This spectrophotometer system allowed either the optical transmittance or optical density (absorbance) of a given sample to be measured in an open air environment as a function of wavelength in the range 190 nm to 820 nm with a resolution of 2 nm. The transmittance is defined as $T = I/I_0$, where I is the light intensity transmitted through a parallel plane sample and I_0 is the intensity of the beam normally incident on the sample. The optical density is defined as $\alpha = \log(1/T)$ where "log" indicates the common (base 10) logarithm. Both the pre- and post-flight optical density spectra of all the samples were taken in the following manner.

Before each sample was placed in the spectrophotometer, a "blank" optical density spectrum was taken of the air. Then the optical density spectrum of the air and the desired sample was taken. Because of the definition of optical density, the air blank spectrum was point-by-point subtracted from the spectrum of the air and sample in order to correct for the presence of the air

in the spectrophotometer optical path. The pre-flight optical density measurements were subtracted from the post-flight measurements in order to obtain the change in optical density due to the space exposure. This procedure facilitates easier recognition of the F-bands. In the figures shown below, the air-corrected optical density spectra are shown in part (a) of the figures, and the change in optical density due to the space exposure are shown in part (b). One pre-flight spectrum was taken for each of the fixed temperature samples: CaF_2 -1 and MgF_2 -1. All other spectra shown and discussed below are averages of at least three different spectra.

It should also be noted that almost all of the pre- and post-flight spectra for all samples had narrow spikes at approximately 580, 600, and 658 nm (the Balmer- α line). All three spikes are features of the spectrophotometer deuterium light source and not of the samples. Because they are not features of the samples, the data points associated with the 580 nm and 658 nm features were removed from the spectra presented below to better facilitate plotting and curve fitting of the spectra. With one exception (sample CaF_2 -1), the 600 nm spike usually disappeared when the pre-flight spectra were subtracted from the post-flight spectra, so the data associated with this feature were not removed from the spectra.

RESULTS

The optical density spectra for sample CaF_2 -1 are shown in figure 1. The optical density spectrum for the masked area is essentially the same as the pre-flight spectrum; it is within the variance seen between different spectra taken on the same day. The exposed surface shows an increased optical density in the UV in addition to an overall increase over the entire spectral range. The feature at 370 nm indicates F-center formation in the exposed side of the sample. This feature is absent in the masked and pre-flight spectra. As discussed above, the spike evident in Figure 1(b) at approximately 600 nm is not a real feature of the sample and can be ignored.

Similar to CaF_2 -1, the optical density spectra for sample CaF_2 -3 show a feature at 370 nm in the exposed side spectrum that is absent in the masked and pre-flight spectra. However, both the masked and exposed optical density are greater than the pre-flight optical density, and in particular, the masked optical density is greater than the exposed. Closer examination of the sample surface revealed that a large portion of the masked area was covered by very fine scratches due to the pre-flight diameter-cutting procedure. These scratches render that region of the sample slightly less transparent than the exposed region due to increased scattering of the light incident on the sample. This increased scattering could certainly be the cause of the increased optical density over the entire spectral range of the masked region of the sample. It should also be noted that CaF_2 -1 was held at a fixed temperature of 60°C during the space exposure while the temperature of CaF_2 -3 was allowed to vary with the ambient environment.

Four different sets of pre- and post-flight optical density spectra were taken for sample CaF_2 -4, and all the post-flight data show a feature at 370 nm that is absent in the pre-flight data. The post-flight optical density is slightly greater than the pre-flight, with the increase qualitatively similar to CaF_2 -1.

The absorption features at the UV end of the spectra shown in figure 1(a) are typical of all the CaF_2 samples. Because the optical density is greatly varying with wavelength in this region near the air/ CaF_2 UV cutoff, the features seen in the corresponding region in figure 1(b) may not be real, even though their magnitudes are of the same order as the F-band observed. However, the F-center appears in a relatively flat, well-behaved section of the exposed-side spectrum, and clearly does not appear in either the pre-flight or masked spectra. Therefore, the observed F-band in CaF_2 is real.

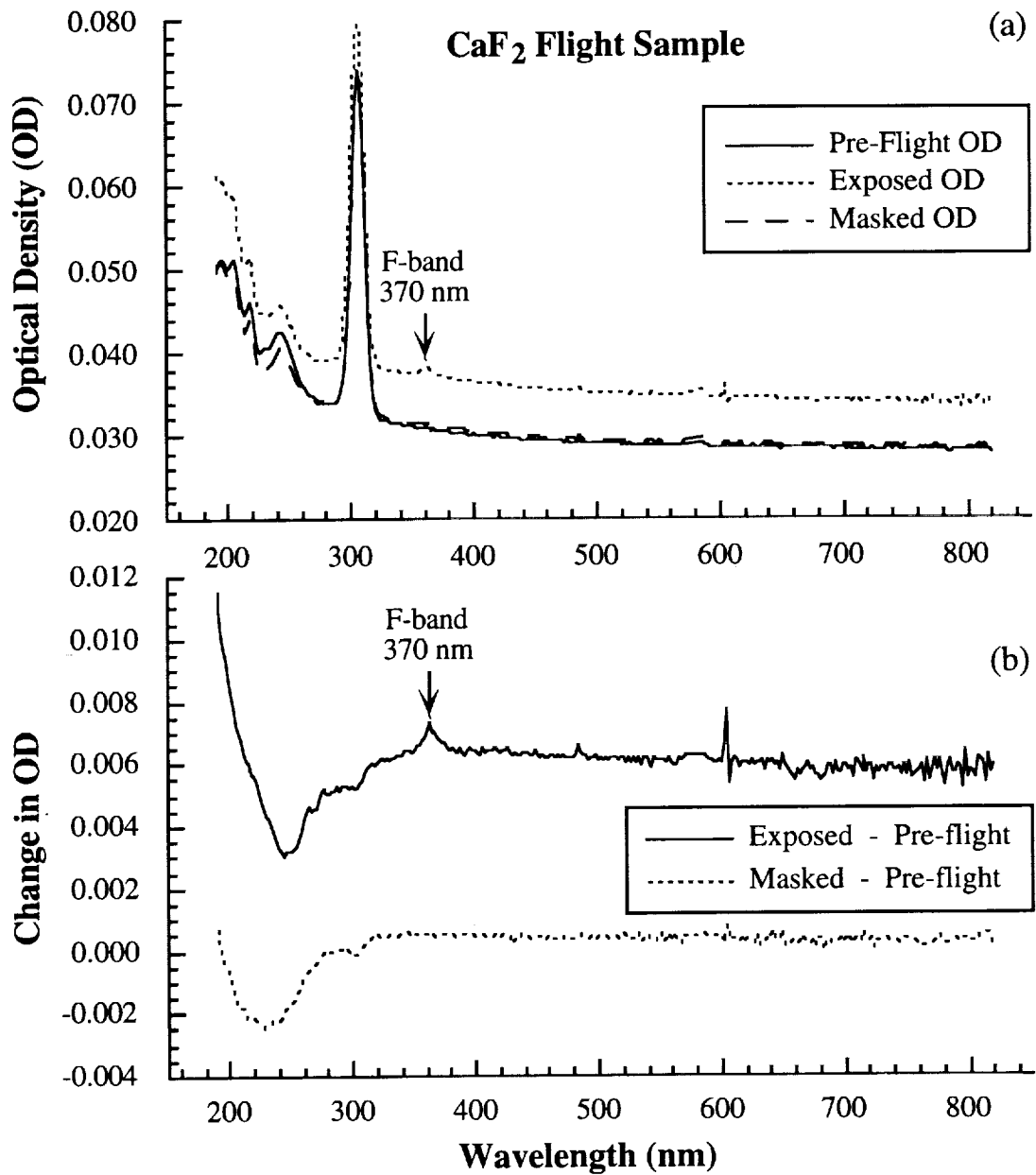


Figure 1. (a) Pre-flight and post-flight optical density (OD) spectra of the exposed and masked areas of sample CaF₂-1. (b) The change in optical density due to the space exposure determined by the difference between the post- and pre-flight spectra from figure (a). The post-flight spectra show the formation of an F-band at 370 nm only on the exposed side of the sample. Sample temperature was held at 60°C during space exposure.

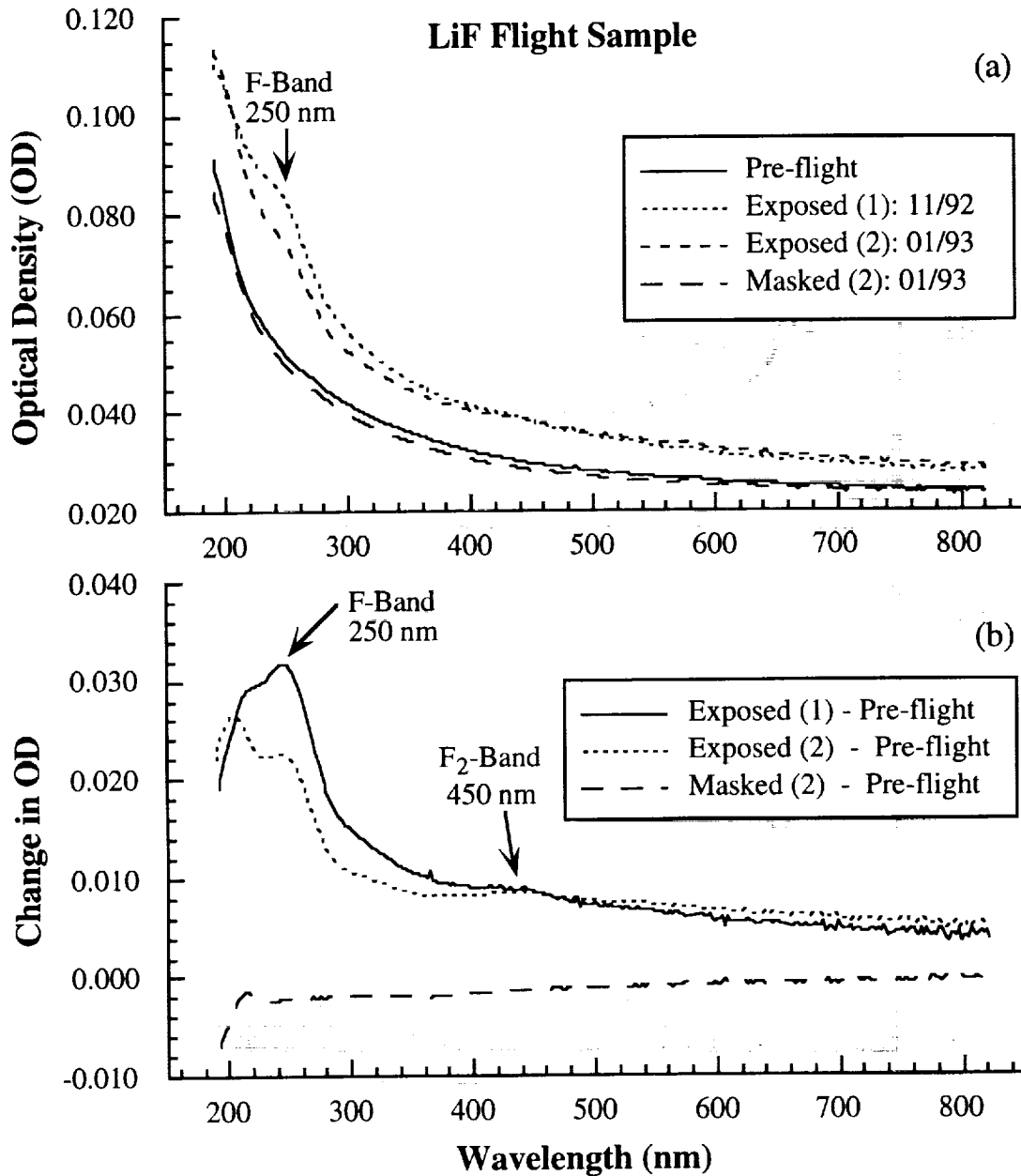


Figure 2. (a) Pre-flight and post-flight optical density (OD) spectra of the exposed and masked areas of sample LiF-2. (b) The change in optical density due to the space exposure determined by the difference between the post- and pre-flight spectra from figure (a). The post-flight spectra show the formation of an F-band at 250 nm and an F₂-band at 450 nm only on the exposed side of the sample. Sample temperature varied with the ambient environment during space exposure.

The optical density spectra for sample LiF-2 are shown in figure 2. The exposed side of the sample shows an increase in optical density as compared to the pre-flight spectrum, while the masked-side spectrum is essentially the same as the pre-flight spectrum. The exposed side shows a prominent F-band at 250 nm, and a small F₂-band is evident at 450 nm. The post-flight spectra taken on different dates clearly show that the F-band is slowly disappearing with time. The absorption peak at 210 nm has been seen before in other experiments where LiF is subjected to

electron bombardment.¹³ A similar F-band envelope in LiF subjected to proton bombardment has been determined to be a complex combination of defect bands involving the presence of impurities and the formation of Li colloids in the crystal.¹⁴

The pre- and post-flight spectra for sample LiF-4 varied greatly with sample orientation in the spectrophotometer and had poor reproducibility. This fact is most probably due to the grinding and polishing described above. In spite of the poor quality of the spectra, an F-band at 250 nm due to space exposure was evident for all sample orientations.

The optical density spectra for sample MgF₂-2 are shown in figure 3. All post-flight spectra for sample MgF₂-1 are very similar to those displayed for MgF₂-2. The exposed side of each sample shows an increased optical density as compared to the pre-flight spectra. Both show a small feature at 230 nm that may be associated with the F-band, which is known to have a peak wavelength of 260 nm in MgF₂ (see table 1). As shown in figure 3(b), the MgF₂-2 exposed side spectrum has a shoulder at approximately 260 nm. This indicates that F-centers may have been formed in that region of the MgF₂ samples exposed to the space environment, but the concentrations are too close to the spectrophotometer detection threshold (approximately 10¹³ F-centers/cm³) to offer conclusive evidence.

Also, the masked side optical density for MgF₂-1 is greater than that of the pre-flight from 200 to approximately 320 nm and is less than the pre-flight for greater wavelengths. The masked optical density for MgF₂-2 is less than the pre-flight optical density at all wavelengths. This difference in the masked side optical densities of the two samples is not yet understood, but it could be at least partially due to a variation in the spectrophotometer lamp intensity and/or room conditions between or during measurements. Both samples were cut from the same crystal, but temperatures of the samples during exposure differed; MgF₂-1 was held at a fixed temperature of 60°C during space exposure while the temperature of MgF₂-2 was ambient.

As mentioned above, sample MgF₂-3 was ground and polished prior to the flight. As with LiF-4, the spectra varied greatly with sample orientation in the spectrophotometer and had poor reproducibility. Consequently, evidence of F-band formation in this sample was inconclusive.

Note that in all cases, the areas of the samples exposed to the LEO environment during the flight show an increased optical density over the entire spectral range. This is evidence for surface metallization although this assumption has not yet been verified by an independent technique. Also, all samples show a greater increase in optical density in the UV portion of the spectra, indicating all of the materials suffered some degree of UV darkening. It also is important to note that none of the samples show any visible signs of darkening or damage.

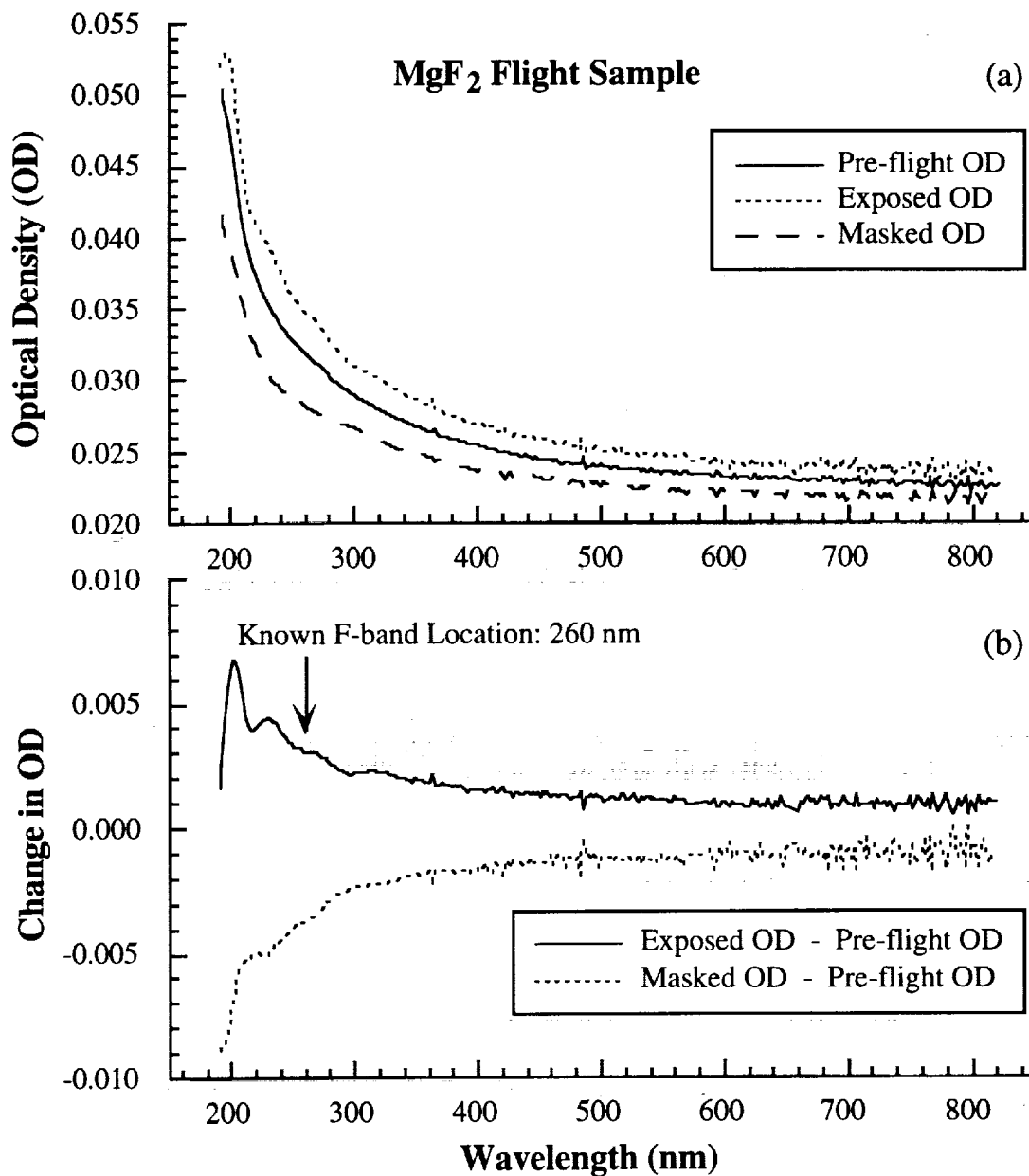


Figure 3. (a) Pre-flight and post-flight optical density (OD) spectra of the exposed and masked areas of sample MgF₂-2. (b) The change in optical density due to the space exposure determined by the difference between the post- and pre-flight spectra from figure (a). The post-flight spectra show absorption features that could be associated with F-center formation only on the exposed side of the sample. Sample temperature varied with the ambient environment during space exposure.

DISCUSSION

F-center formation in alkali-halide crystals such as LiF has been studied in detail for many years, and the shape of the F-band in optical absorption spectra is well-known to be Gaussian, or nearly Gaussian.^{8, 15} An order of magnitude estimate of the average F-center concentration in sample LiF-2 can be made using the following form of the modified Smakula formula for a Gaussian band shape:^{8, 16}

$$Nf = 0.87 \times 10^{17} \frac{n}{(n^2 + 2)^2} \mu_m W$$

where N is the number of defects per cubic centimeter, f is the oscillator strength, n is the index of refraction in the spectral region of the band, μ_m is the absorption coefficient at the band peak expressed in cm^{-1} , and W is the full width at half maximum of the band expressed in electron volts.

The absorption coefficient is defined as $\mu = (1/d) \ln(1/T)$, where d is the sample thickness and "ln" indicates the natural (base e) logarithm. Consequently, the absorption coefficient is related to the optical density, as measured by the spectrophotometer, by $\mu = 2.303 \alpha/d$.

The F-band peaks and full widths for sample LiF-2 were determined from fits of multiple Gaussians with a second order polynomial background to the difference between the exposed and pre-flight optical density spectra (as shown in figure 2b). The F-band has a constant peak wavelength and width at a given temperature,⁵⁻⁸ so only the peak height should change as a function of time. Therefore, the final fit of each spectrum was made with the center wavelength and width of the F-band fixed at the average value achieved from initial fits. The oscillator strength is nearly unity for F-bands^{15, 17} and the index of refraction of LiF is 1.420 at the peak wavelength of the F-band.¹⁸ Therefore, the average F-center concentrations in sample LiF-2 due to space exposure can be calculated using the Smakula formula above. For the 0.4 cm thick LiF-2 sample, the results of the curve fits are tabulated in table 3.

Table 3. *F-center concentrations in sample LiF-2.*

Parameter	Spectrum 11/92	Spectrum 01/93	Spectrum 08/93
λ_0 (nm)	245.7	245.7	245.7
μ_m (cm^{-1})	0.1031	0.0757	0.0721
W (eV)	0.953	0.953	0.953
N (cm^{-3})	$7.53 \cdot 10^{14}$	$5.53 \cdot 10^{14}$	$5.28 \cdot 10^{14}$

These concentrations are about 5 orders of magnitude smaller than the typical concentrations induced by low-energy electron bombardment.¹³ If we assume 100 eV is needed to create each stable F-center,¹⁹ then the energy absorbed by sample LiF-2 in the formation of the F-band was approximately 7.53×10^{16} eV/ cm^{-3} for the 11/92 spectrum.

The interactions of low-energy electrons, protons, and heavy particles with an alkali-halide crystal are confined to the near surface bulk of the crystal. If the energy of the incident particles is high enough to allow F-center formation, the resulting F-center distributions will greatly vary

with depth in the crystal. Bombardment of alkali-halide crystals by photons with energies well above the band gaps will produce similar distributions. However, photons with energies near the excitonic absorption edge, where the sample is still largely transparent, will deposit their energy fairly uniformly throughout the sample bulk, leading to a relatively uniform F-center distribution.

When alkali halides, such as LiF, are bombarded by electrons with energies of a few hundred eV, clusters of lithium atoms form on the sample surface.^{9, 13, 20} This surface metallization is observed as a very broad absorption band that first appears near the F₂-band and shifts to longer wavelengths as the clusters increase in size. The absorption spectra for sample LiF-2 do not exhibit a broad metal peak, but any lithium clusters that might have formed on the surface of LiF-2 would have been most likely altered by exposure to atomic oxygen during the flight or air during the post-flight retrieval. Therefore, absence of a broad metal peak does not rule out electron bombardment as the cause of the F-center formation.

However, typical LEO electron densities range from 10⁵ to 10⁶ cm⁻³ with an average energy of 0.1 eV.²¹ Electrons and protons in the keV energy range were present in the EOIM-III flight environment,* but fluxes were several orders of magnitude lower than the calculated UV/VUV fluxes. Therefore, electron, proton, and other ion fluences were far too small to be primary causes of the F-center formation observed. Even though the samples were exposed to significant atomic oxygen fluxes, the collisional energies are most probably far below the threshold for physical sputtering,²² and are too low to cause the ionization necessary for F-center formation.

The band gap energy of pure LiF is 13.6 eV,¹⁸ and it is possible to create the vacancies and interstitials that lead to F-centers in LiF crystals by irradiating them with ultraviolet light with energies down to the excitonic region of the absorption spectrum⁸, which begins at approximately 11 eV for LiF.²³ The laboratory experiments discussed below also indicate that photons with energies as low as Lyman- α (121.5 nm - 10.2 eV) can form F-centers in the LiF samples of this study. As mentioned above, preliminary solar UV/VUV fluxes/fluences were calculated for the STS-46 flight by using a detailed calculation to estimate the accumulated direct solar flux on the EOIM-III payload.¹² The results for photons with energies sufficient to cause F-center formation in LiF are tabulated in Table 4.

Table 4. STS-46 solar UV exposure history for photon energies great enough to cause F-center formation in LiF.¹¹

Mission Days	Sun Hours	Solar UV Flux (mW/cm ²)	
		121.5 nm	119-10 nm
0 - 2.0	5.8	7.1·10 ⁻⁴	3.3·10 ⁻⁴
3.0 - 4.0	6.8	7.5·10 ⁻⁴	3.7·10 ⁻⁴
4.0 - 5.8	10.4	7.5·10 ⁻⁴	3.6·10 ⁻⁴
5.8 - 6.0	0.3	7.5·10 ⁻⁴	3.6·10 ⁻⁴
6.0 - 7.0	4.4	7.7·10 ⁻⁴	3.7·10 ⁻⁴
7.0 - 8.0	2.9	7.8·10 ⁻⁴	3.8·10 ⁻⁴

The total integrated fluence from these data, normalized to the exposed volume of sample LiF-2, is 1.0·10¹⁹ eV/cm³. This is approximately a factor of 130 greater than the estimated energy needed to form the F-band observed in the 11/92 absorption spectrum for this sample. It also should be noted that during the EOIM-III operation period at 123-124 nmi a significant change in solar activity occurred.¹⁰ Since the calculated solar exposure is based on typical solar

* Donald Hunton, private communication

radiation behavior in LEO, it is very likely the EOIM-III samples were subjected to a significantly higher solar UV/VUV radiation exposure than was calculated. Experience with electron bombardment of alkali halides has shown that production efficiency of stable F-centers is a few percent. Given this fact, the fluence and F-center concentrations discussed above are very consistent. Therefore, solar UV/VUV exposure is the most likely cause of the observed F-band in sample LiF-2, and consequently, in all the CMASS/NASA samples.

For photon energies above approximately 12 eV (103 nm), LiF has an average absorption coefficient of approximately $0.5 \cdot 10^6 \text{ cm}^{-1}$ [23] which corresponds to an absorption length (or penetration depth) of 200 Å. Consequently, F-centers produced in LiF by photons with energies above 12 eV would be limited to the near surface bulk, and average concentrations of 10^{14} F-centers/cm³ would actually represent local concentrations on the order of 10^{19} F-centers/cm³. Such concentrations are sufficient to produce coloration that is noticeable to the unaided eye. No visible signs of any coloration or damage was evident in any of the CMASS/NASA samples flown on EOIM-III. Also, it is well known that the solar UV spectrum is dominated by Lyman- α and longer wavelengths. Therefore, the F-centers observed in the CMASS/NASA samples are most likely due to solar UV photons with energies below 12 eV. If this is indeed the case, then the F-centers will be distributed somewhat uniformly throughout the bulk of the samples. Measurements of the actual F-center spatial distributions will clarify this issue, and experiments are currently being set up to perform such measurements on the samples.

To test the hypothesis that solar UV/VUV exposure caused the F-center formation in all the CMASS/NASA samples, UV/VUV exposures were performed in the laboratory using deuterium lamps. Control samples CaF₂-2 and LiF-3 were masked in an identical fashion as the flight samples, placed in a vacuum chamber, and exposed to approximately 100 solar equivalent hours. With the same spectrophotometer used for the flight samples, optical absorption spectra were taken of samples CaF₂-2 and LiF-3 both before and after the laboratory UV/VUV exposure. Figure 4 shows the change in optical density due to the UV exposure as a function of wavelength for samples CaF₂-2 (figure 4a) and LiF-3 (figure 4b). The spectra are similar to the applicable flight sample spectra, and F-bands in the exposed area of each control sample can clearly be seen. Also, as with the flight samples, no visible darkening, coloration, or damage is evident in these samples.

The deuterium lamps used for these experiments have MgF₂ windows which transmit very little light at wavelengths shorter than Lyman- α (121.6 nm).²⁴ Therefore, the small F-band evident in sample LiF-3 justifies the inclusion of photon fluxes at Lyman- α in the above analysis associated with Table 4. The differences between the control and flight sample spectra are most probably due to the fact that a deuterium lamp does not exactly duplicate the solar spectrum, especially in the spectral range of interest. However, the fact that F-centers were formed in the control samples by photons limited to Lyman- α wavelengths or longer is significant, because photon fluxes in this region dominate the solar UV spectrum. Consequently, this laboratory experiment provides very strong evidence that solar UV radiation was the primary cause of the F-center formation in the flight samples.

The formation of F-bands in optical materials exposed to the space environment has prompted the re-examination of optical absorption spectra from previous shuttle flight experiments. Figure 5 shows pre- and post-flight optical density spectra for a LiF sample flown on STS-4, which was of similar duration to STS-46. The post-flight spectrum clearly shows an F-band at 250 nm, and the calculated F-center concentration is approximately $5 \cdot 10^{14}$ F-centers/cm⁻³, a concentration very similar to that observed in EOIM-III sample LiF-2.

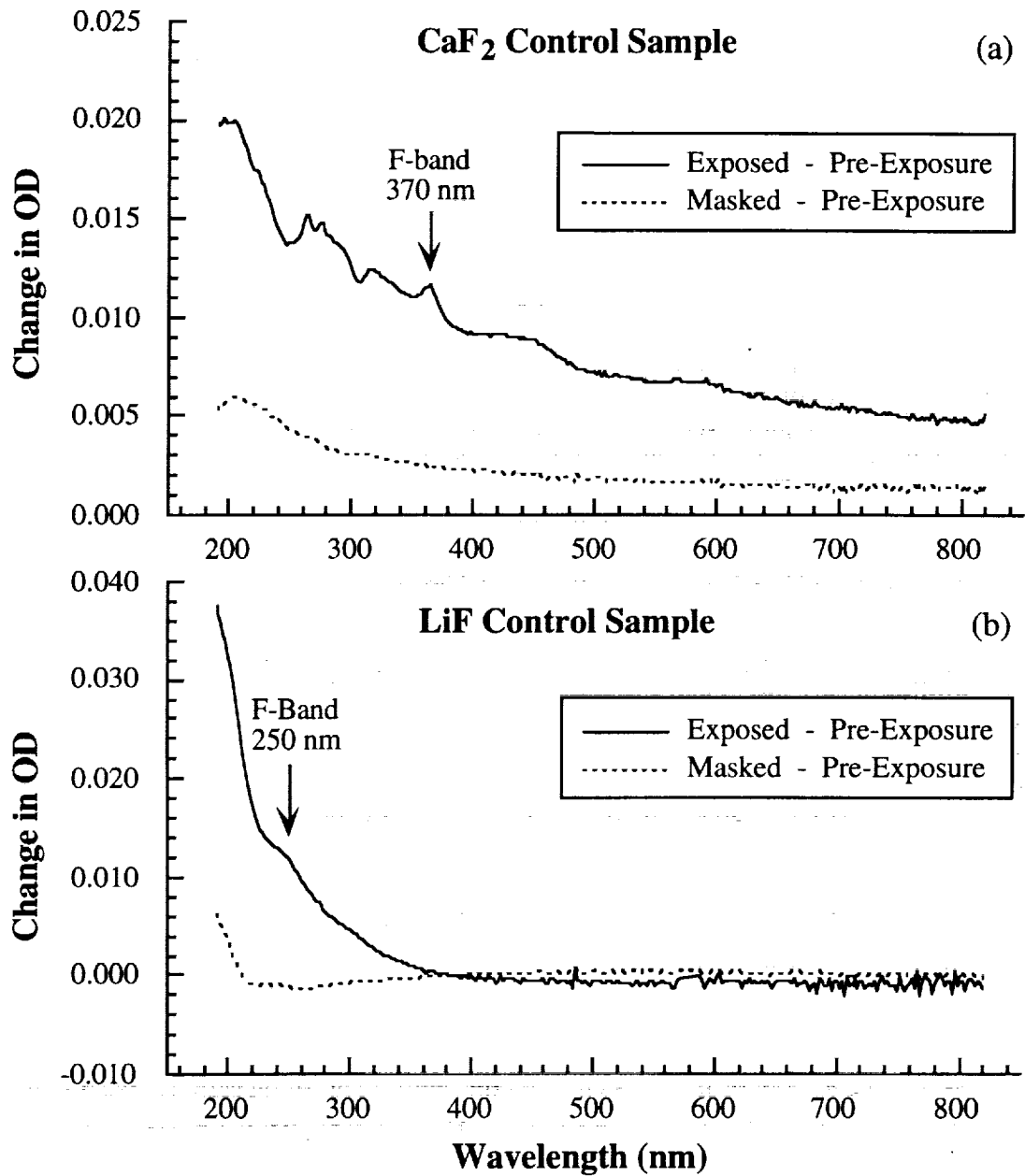


Figure 4. The change in optical density due to VUV exposure in the laboratory of control samples (a) CaF₂-2 and (b) LiF-3. The laboratory VUV exposures show similar defect formation as that observed in the EOIM-III flight samples.

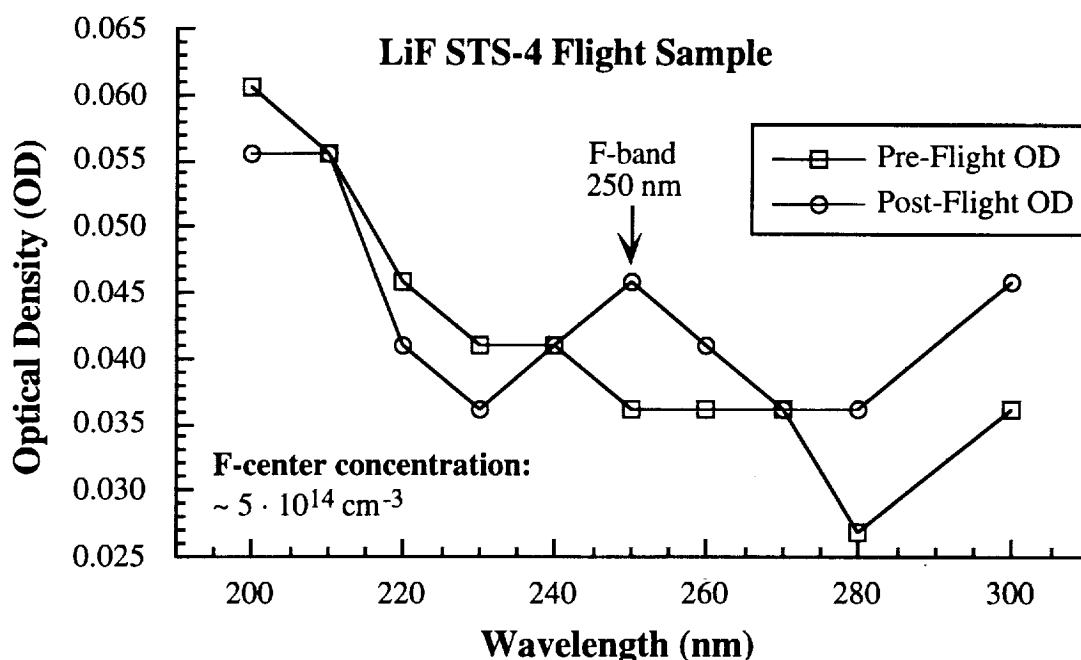


Figure 5. Pre- and post-flight optical density spectra for a LiF sample flown on space shuttle flight STS-4. The spectra show that F-centers were formed due to the space exposure.

CONCLUSIONS

Pre- and post-flight optical absorption measurements of CaF₂ and LiF samples flown by CMASS/NASA on EOIM-III clearly indicate F-center formation in these samples due to space exposure. The space-exposed MgF₂ samples show some UV absorption features that could be associated with F-center formation, but the evidence is less compelling than with the CaF₂ and LiF samples. All samples also exhibited UV darkening as well as increased optical density throughout the entire spectral range of measurement. This overall darkening is evidence for surface metallization with subsequent oxidation due to the atomic oxygen environment, although this assumption has not yet been verified by an independent technique.

The F-center formation in the LiF samples was much more pronounced than in either the CaF₂ or MgF₂ samples. This is consistent with previous laboratory experiments,²⁵ and what is known about the ability to produce F-centers in alkali halides as compared to alkaline-earth fluorides.⁷ Estimates of the F-center concentration in sample LiF-2 and the energy available in solar VUV radiation to create the F-centers are consistent. Laboratory experiments to simulate solar UV exposure caused F-center formation in control samples similar to that observed in flight samples. Because of these results and what is known about the EOIM-III radiation environment, solar VUV radiation exposure is most likely the primary cause of the F-center formation. Re-examination of STS-4 flight experiment data shows F-center formation in LiF similar to that observed on EOIM-III.

These results represent the initial set of post-flight examinations being planned for these samples; the next tests to be performed are currently being determined. Emphasis will be placed on determining F-center spatial distributions and detailed studies of how F-center formation is affected by crystal impurities. This information is not only of fundamental scientific interest in

understanding microscopic defect dynamics, but also could lead to schemes for radiation hardening of optical materials against darkening and damage.

It has been established that point defect formation leads to darkening and damage of optical materials. The results presented here show that the precursors to darkening and damage can be quantitatively studied in materials exposed to the space environment before any visible darkening or damage occurs. This further emphasizes the importance of careful selection and development of optical materials for space experiments.

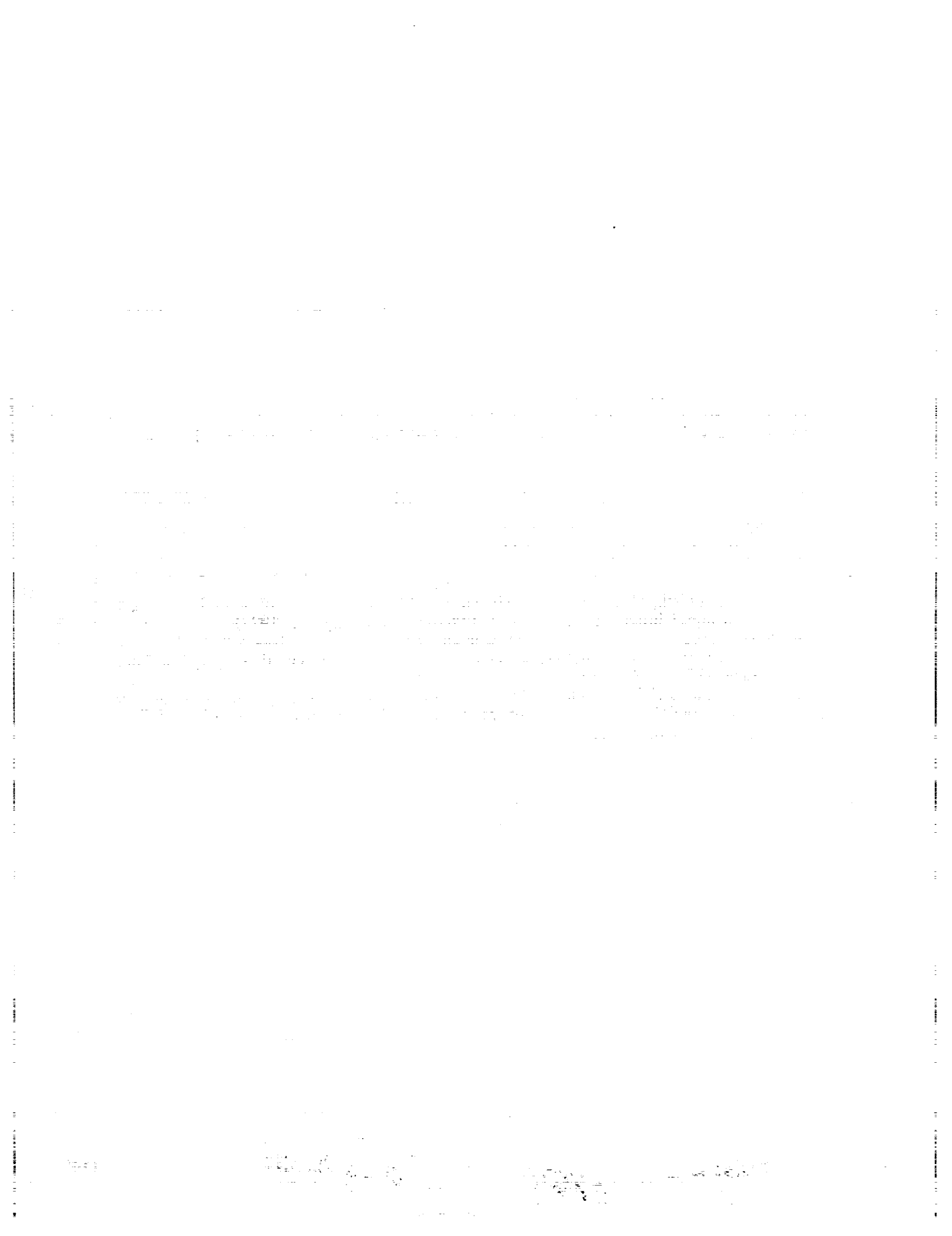
ACKNOWLEDGMENTS

The authors wish to thank L. Reinisch for the use of his spectrophotometer, and P. Gray for his assistance in performing the laboratory UV exposure experiments. The authors also wish to thank S. Espy, I. Urazgil'din, W. Heiland, and P. Nordlander for helpful discussions. This work was supported in part by the National Aeronautics and Space Administration through the Tennessee Space Grant Consortium, NASA Contract No. 4-20-630-3581, and the Office of Naval Research under Contracts No. N00014-87-C-0146, No. N00014-91-C-0109, and Grant No. N00014-91-J-4040.

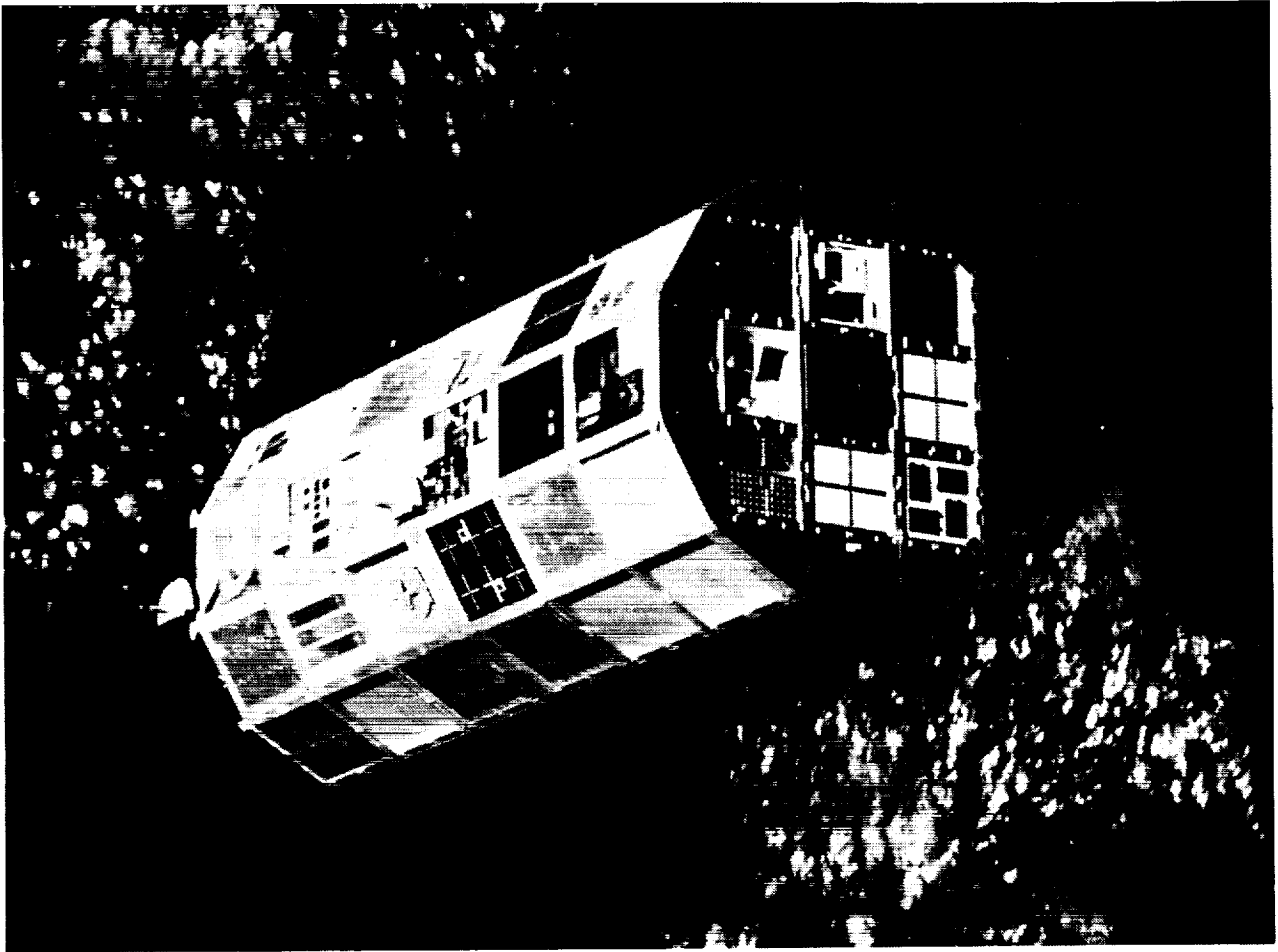
REFERENCES

1. L. J. Leger, "Oxygen Atom Reaction with Shuttle Materials at Orbital Altitudes - Data and Experiment Status," AIAA paper AIAA-83-0073, AIAA 21st Aerospace Sciences Meeting, January 10-13, 1983, Reno, NV.
2. J. T. Visentine, L. J. Leger, J. F. Kuminecz, and I. K. Spiker, "STS-8 Atomic Oxygen Effects Experiment," AIAA paper AIAA-85-0415, AIAA 23rd Aerospace Sciences Meeting, January 14-17, 1985, Reno, NV.
3. L. J. Leger, J. T. Visentine, and J. A. Schliesing, "A Consideration of Atomic Oxygen Interactions with Space Station," AIAA paper AIAA-85-0476, AIAA 23rd Aerospace Sciences Meeting, January 14-17, 1985, Reno, NV.
4. P. N. Peters, J. C. Gregory, and J. T. Swann, "Effects on optical systems from interactions with oxygen atoms in low earth orbits," *Appl. Opt.* **25** (8), 1290 (15 April 1986).
5. W. B. Fowler, editor, *Physics of Color Centers*, Academic Press, New York, 1968.
6. A. Van Den Bosch, " γ -Radiolysis of LiF," *Rad. Eff.* **19**, 129 (1973).
7. Y. Farge and M. P. Fontana, *Electronic and Vibrational Properties of Point Defects in Ionic Crystals*, North-Holland Publishing Company, Amsterdam, 1979.
8. F. Agullo-Lopez, C. R. A. Catlow, and P. D. Townsend, *Point Defects in Materials*, Academic Press, London, 1988.
9. See several of the articles and their associated references in "Damage to Space Optics and Properties and Characteristics of Optical Glass," *Proceedings of SPIE, Volume 1761*, edited by J. A. Breckinridge and A. J. Marker III (1992).
10. L. J. Leger, S. L. Koontz, J. Visentine, and D. Hunton, "An Overview of the Evaluation of Oxygen Interaction with Materials - Third Phase (EOIM-III) Experiment: Space Shuttle Mission 46," AIAA paper AIAA 93-0497, AIAA 31st Aerospace Sciences Meeting, January 11-14, 1993, Reno, NV.
11. L. J. Leger, "Evaluation of Oxygen Interactions with Materials III (EOIM-III) Flight Experiment Update," NASA Johnson Space Center Memorandum ES5-93-118, July 2, 1993.

1993. The latest atomic oxygen fluence data was relayed to EOIM-3 community by S.L. Koontz, June 1994
12. S. L. Koontz, L. J. Leger, S. L. Rickman, J. B. Cross, C. L. Hakes, and D. T. Bui, "Evaluation of Oxygen Interactions with Materials III - Mission and Induced Environments," presented at the *Third LDEF Post-Retrieval Symposium*, Williamsburg, VA (November 8-12, 1993).
 13. N. Seifert, H. Ye, D. Liu, R. G. Albridge, A. V. Barnes, N. Tolk, W. Husinsky, and G. Betz, "Simultaneous measurements of transmission optical absorption and electron stimulated Li desorption on LiF crystals," *Nucl. Instrum. Meth. Phys. Res.* **B72**, 401 (1992).
 14. R. A. Wood and P. D. Townsend, "An investigation of the structure of the F-band and envelope in LiF," *Nucl. Instrum. Meth.* **B65**, 502-506 (1992).
 15. J. H. Schulman and W. D. Compton, *Color Centers in Solids*, Pergamon Press, Oxford, 1963.
 16. B. Henderson and A. E. Hughes, editors, *Defects and Their Structures in Nonmetallic Solids*, Plenum Press, New York, 1976.
 17. J. J. Markham, *F- Centers in Alkali Halides*, Academic Press, New York, 1966.
 18. P. Klocek, editor, *Handbook of Infrared Optical Materials*, Marcel Dekker, Inc., New York, 1991.
 19. A. E. Hughes and A. B. Lidiard, AERE-R13319, Harwell Report HL89/1047, 1989.
 20. Q. Dou and D. W. Lynch, "Electron-Irradiation-Induced Structural and Compositional Changes on Alkali Halide Surfaces," *Surf. Sci.* **219**, L623 (1989).
 21. "Space Station Natural Environment Definition for Design," Johnson Space Center, Houston, TX, JSC 30425, Jan. 1987.
 22. R. Behrisch, editor, *Sputtering by Particle Bombardment II*, Springer-Verlag, Berlin, 1983.
 23. R. -P. Haelbich, M. Iwan, E. E. Koch, editors, "Optical Properties of Some Insulators in the Vacuum Ultraviolet Region," *ZAED Physik Daten* (August 1, 1977).
 24. J. H. Moore, C. C. Davis, and M. A. Coplan, *Building Scientific Apparatus: A Practical Guide to Design and Construction* (2nd edition), Addison-Wesley Publishing Co., Inc., Redwood City, CA, 1989.
 25. D. H. Heath and P. A. Sacher, "Effects of a Simulated High-Energy Space Environment on the Ultraviolet Transmittance of Optical Materials between 1050 Å and 3000 Å," *Appl. Opt.* **5** (6), 937 (June 1966).



SYSTEMS



84-04319

PRECEDING PAGE BLANK NOT FILMED

1147

1. Introduction

2. Methodology

3. Results

4. Discussion

5. Conclusion

6. References

7. Appendix

8. Acknowledgements

9. Contact Information

10. Disclaimer